Improved Polarimetric Calibration for Atmospheric Radars

DMITRI N. MOISSEEV,* CHRISTINE M. H. UNAL, HERMAN W. J. RUSSCHENBERG, AND LEO P. LIGTHART

IRCTR, Delft University of Technology, Delft, Netherlands

(Manuscript received 16 August 2001, in final form 27 May 2002)

ABSTRACT

Polarization properties of radar waves that are scattered from atmospheric objects are of great interest in meteorological studies. However, polarimetric radar measurements are often not sufficiently accurate for retrieving physical properties of targets. To compensate for errors, radar polarimetric calibration is applied. Typical calibrations are performed based on measurements of point targets with known scattering matrices located in the boresight of the antenna. Such calibration takes into account the polarization state of the antenna pattern only at one point. Since radar measurements of atmospheric phenomena involve distributed targets that fill the full antenna beam, point target radar calibrations are inadequate for meteorological studies.

This paper explains in detail the effects of the complete antenna patterns on weather echoes. It is shown that the conventional polarimetric calibration can be significantly improved by incorporating light-rain ($<$20 dBZ) zenith-pointing measurements into the calibration procedure. As a result, the sensitivity of cross-polar measurements can be improved by 7 dB on average. Also it is shown that the bias in co-cross-polar correlation coefficient can be reduced.

1. Introduction

During recent years there has been a growing interest in the use of radar polarimetry for atmospheric studies. This has resulted in the use of various polarimetric parameters for the characterization of the meteorological media (Zrnić and Ryzhkov 1999). However, little attention has been given to the polarimetric calibration of atmospheric radars. Current calibration techniques are based on the measurement of known point targets. This approach is based on the assumption that the polarimetric measurements with the radar can be described by the polarimetric properties of only one point of the radar antenna pattern. However, atmospheric radars most of the time are used for studies of extended radar objects and thus full antenna pattern information must be taken into account.

The main goal of using calibration methods based on point-target measurements is to estimate the distortion matrices (McCormick 1981), which characterize the transmit and receive channels of the system. Many different approaches are described in the literature to retrieve these distortion matrices. The main difference between them lies in the assumptions which are used in order to simplify the calibration procedure. It was shown by Sarabandi and Ulaby (1990) that if the antenna system and two orthogonal channels of the radar system are modeled as a four-port passive network, the calibration can be simplified to the measurement of a metallic sphere. Another approach is to assume a good polarization isolation of the system ($>$25 dB); then the polarimetric calibration can be done by using a metallic sphere and an unknown highly depolarizing target (Sarabandi et al. 1990). The use of the assumption of reciprocity of the antenna system was demonstrated by Unal et al. (1994), and because of this assumption the polarimetric calibration can be carried out by using a single rotatable dihedral corner reflector. The use of weather echoes for calibration was demonstrated by Hubbert and Bringi (2001). However, in this paper the point target calibration formalism was also employed as the basis for the calibration procedure.

In this article we analyze the errors that are implied by the point target calibration formalism. Based on this analysis a correction method for existing calibration procedures is proposed. It is demonstrated that by applying this correction we can obtain more accurate cross-polar measurements. This new polarimetric calibration procedure is demonstrated using a set of precipitation measurements collected with the Delft Atmospheric Research Radar (DARR). The DARR description is given by Ligthart and Nieuwkerk (1980).

* Current affiliation: DEOS, Delft University of Technology, Delft, Netherlands.

Corresponding author address: Dr. Dmitri N. Moisseev, DEOS, Delft University of Technology, Thijsseweg 11, 2629 JA Delft, Netherlands.
E-mail: d.moisseev@citg.tudelft.nl

2. Point target polarimetric calibration

For an ideal polarimetric system, the measured scattering matrix of an object, **M**, is identical to the actual scattering matrix, **S**. However, in real radar systems these matrices are different. Usually this difference is explained by the divergence of the expected transmit and receive polarization states from the actual ones. For example, a radar transmit (or receive) basis that is treated as a linear $h - v$ basis is in reality a nonorthogonal basis with polarization vectors that are slightly elliptical. In this case the measured scattering matrix can be represented as

$$\mathbf{M} = \mathbf{RST}, \tag{1}$$

where **R** and **T** are the antenna distortion receive and transmit 2×2 matrices, or, in other words, the matrices that transform the desired polarimetric basis into the actual antenna basis. This equation provides the basis for the point target polarimetric radar calibration. It can be seen that if no assumptions are made about the **R** and **T** matrices, three known point targets are required to retrieve all elements of the distortion matrices.

Following the assumption used by Unal et al. (1994) and Hubbert and Bringi (2001) that the radar can be considered to be reciprocal ($\mathbf{M}^{\mathrm{T}} = \mathbf{M}$), the formulation can be simplified as

$$\mathbf{M} = \mathbf{T}^{\mathrm{T}}\mathbf{ST}, \tag{2}$$

where

$$\mathbf{T} = T_{11} \cdot \begin{bmatrix} 1 & \delta_2 \\ \delta_1 & f \end{bmatrix} \tag{3}$$

and δ_1, δ_2 represent coupling terms between the radar polarization channels, f is the one-way copolar channel imbalance, and T_{11} is the coefficient that combines the absolute calibration constant and the radio wave propagation coefficient. It should be noted that since we are interested only in relative polarimetric calibration, the coefficient T_{11} is not considered in our discussion for the sake of simplicity.

Using the formulation (2) and (3) and taking into account that the matrices **M** and **S** are symmetric, we can rewrite (2) as

$$\mathbf{m} = \begin{bmatrix} 1 & 2\delta_1 & \delta_1^2 \\ \delta_2 & f + \delta_1\delta_2 & f\delta_1 \\ \delta_2^2 & 2f\delta_2 & f^2 \end{bmatrix} \cdot \mathbf{s}, \tag{4}$$

where **s** and **m** are vector representations of the matrices **M** and **S**,

$$\mathbf{s} = [S_{hh}\ S_{hv}\ S_{vv}]^{\mathrm{T}} \quad \text{and} \quad \mathbf{m} = [M_{hh}\ M_{hv}\ M_{vv}]^{\mathrm{T}}.$$

It is common to use the polarimetric covariance matrix $\mathbf{C} = \langle \mathbf{s} \cdot \mathbf{s}^{+} \rangle$ for the description of atmospheric targets (Santalla et al. 1999; Ryzhkov 2001); here $^{+}$ is the Hermitian transpose operator and $\langle\ \rangle$ denotes an ensemble average. Using a general relationship

$$\mathbf{A} = \mathbf{BCD} \rightarrow \mathbf{a} = (\mathbf{B} \otimes \mathbf{D}^{\mathrm{T}})\mathbf{c},$$

where **A**, **B**, **C**, and **D** are $n \times n$ matrices, and **a**, **c**, are n^2 vector representations of **A** and **C** formed by stacking the rows of the matrices, the calibrated covariance matrix **C** can be obtained from (4) as follows:

$$\mathbf{c}_m = \mathbf{Dc}_s, \tag{5}$$

where $\mathbf{c}_m$ and $\mathbf{c}_s$ are the vector representations of the measured and actual object's covariance matrices and **D** is the system distortion matrix, which is defined as

$$\mathbf{D} = \begin{bmatrix} 1 & 2\delta_1 & \delta_1^2 \\ \delta_2 & f + \delta_1\delta_2 & f\delta_1 \\ \delta_2^2 & 2f\delta_2 & f^2 \end{bmatrix} \otimes \begin{bmatrix} 1 & 2\delta_1 & \delta_1^2 \\ \delta_2 & f + \delta_1\delta_2 & f\delta_1 \\ \delta_2^2 & 2f\delta_2 & f^2 \end{bmatrix}^{*}. \tag{6}$$

Here $\otimes$ denotes the Kronecker matrix product and * denotes complex conjugation.

Assuming we know f, δ_1, and δ_2, one can invert (5) to obtain the calibrated covariance matrix of a radar object. However, this approach is based on the assumption that it suffices to estimate the distortion matrix at only one point of the antenna pattern. This approach can be erroneous, especially for atmospheric studies, where the complete antenna pattern plays a role in the radar measurement.

3. Effect of the complete antenna patterns on atmospheric measurements

a. Polarimetric measurements of distributed targets

For a distributed target measurement, the measured scattering matrix can be related to the target scattering matrix by (Blanchard and Jean 1983; Doviak and Zrnić 1993):

$$\mathbf{M} = \iint [f_r(\theta, \phi)]\tilde{\mathbf{S}}(\theta, \phi)[f_t(\theta, \phi)] \sin\theta\, d\theta\, d\phi, \tag{7}$$

where

$$[f_i(\theta, \phi)] = \begin{bmatrix} f_{hh}(\theta, \phi) & f_{hv}(\theta, \phi) \\ f_{vh}(\theta, \phi) & f_{vv}(\theta, \phi) \end{bmatrix} \quad \text{with } i = r, t$$

is the receive (or transmit) distortion matrix whose elements are antenna patterns for all polarization states and $\tilde{\mathbf{S}}(\theta, \phi)$ is the scattering matrix of an extended radar target for the azimuth angle θ and the elevation angle ϕ. This formulation gives the most general description of the influence of the radar system on polarimetric measurements. From (7) it follows that in order to perform an accurate polarimetric radar calibration, one requires knowledge of eight 2D antenna patterns (four if the reciprocity assumption of the antenna system is used). However, measuring antenna patterns accurately is complicated and time consuming, and not an option for most atmospheric radars. That is why it is important

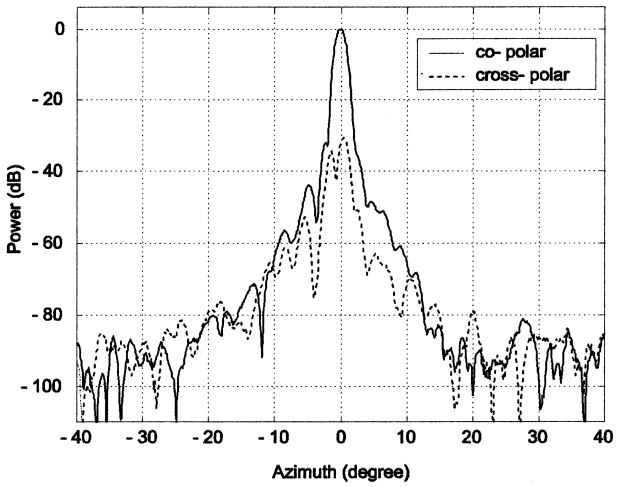

FIG. 1. Two-way antenna patterns (45° plane). The solid line is the copolar pattern and the dashed line is the cross-polar pattern.

to examine how the antenna patterns influence the polarimetric measurements of atmospheric objects and what can be done to reduce this effect.

b. Copolar channel imbalance

The channel imbalance f is an important parameter; it can be seen from (2) and (3) that for radars with good polarization isolation (small δ_1, δ_2) the accuracy of the measured differential reflectivity ($Zdr = \langle|M_{hh}|^2\rangle/\langle|M_{vv}|^2\rangle$) is directly related to f.

In order to determine how the complete antenna pattern influences *Zdr* measurements, we used the antenna patterns for DARR (see Fig. 1). Coherent measurements of the antenna patterns were available in principal and 45° planes (Aubry and Zijderveld 1999). The effects of the antenna patterns were best illustrated using 45° plane measurements, in conjunction with the assumption of rotational symmetry. Using (7) we have estimated the measured *Zdr* value for a target with $Zdr = 0$ dB. Based on these calculations we have found that the difference between copolar polarization channels due to the use of full antenna patterns is small and gives an uncertainty in *Zdr* measurements of about 10^{-2} dB.

Due to uncertainties in the antenna pattern model and in the antenna measurements, especially for far sidelobes, this estimation does not give us the exact value of the influence of the complete antenna patterns on f. However, it does give us an estimate of the order of magnitude of this influence. Thus for most atmospheric studies the required *Zdr* accuracy of about 0.1 dB can be achieved by applying a point target polarimetric calibration.

c. Polarization isolation for a distributed target

The other important characteristic of an antenna system is the polarization isolation. The polarization isolation defines how pure the polarization state of a radar is. For atmospheric studies the polarization isolation of the radar determines the minimum possible measured linear depolarization ratio values ($Ldr = \langle|M_{vh}|^2\rangle/\langle|M_{hh}|^2\rangle$). If the point calibration notation is used, the polarization isolation ρ_a is given by

$$\rho_a = \frac{\langle|M_{hh}|^2\rangle}{\langle|M_{vh}|^2\rangle} = \frac{|1 + \delta_1^2|^2}{|\delta_2 + f\delta_1|^2} \simeq |\delta_2 + f\delta_1|^{-2}, \quad (8)$$

where $\langle|M_{hh}|^2\rangle$ and $\langle|M_{vh}|^2\rangle$ are averaged measured powers of *hh*, and *vh* elements of the scattering matrix of a polarimetrically isotropic nondepolarizing target ($\langle|S_{vh}|^2\rangle = 0$, $\langle|S_{hh}|^2\rangle = \langle|S_{vv}|^2\rangle$). It can be seen that the smallest measurable *Ldr* value is fully determined by the antenna isolation value, namely $Ldr_{\min} = 1/\rho_a$. Based on the point target calibration (Unal et al. 1994) it was determined that this value is 33 dB for DARR.

However, many atmospheric measurements with DARR showed that this value is never achieved and the minimum measured *Ldr* value is only −27.5 dB. This *Ldr* value does not represent the characteristic of atmospheric echoes, but the antenna polarization isolation. This difference between the predicted and measured polarization isolation was first described by Blanchard and Jean (1983). It was shown that this discrepancy is explained by the way in which the polarization isolation is determined: whether it is estimated from single point (boresight) measurements or by taking into account the complete antenna patterns.

From (7) and (8), we can define the polarization isolation for an extended target as

$$\tilde{\rho}_a = \frac{\langle|M_{hh}|^2\rangle}{\langle|M_{vh}|^2\rangle}$$

$$\langle|M_{hh}|^2\rangle \simeq \left\langle \left| \int \tilde{S}_{hh}(\theta, \phi) \cdot f_{thh}(\theta, \phi) f_{rhh}(\theta, \phi)\, d\Omega \right|^2 \right\rangle$$

$$\langle|M_{vh}|^2\rangle \simeq \left\langle \left| \int \tilde{S}_{hh}(\theta, \phi) \cdot f_{thh}(\theta, \phi) f_{rvh}(\theta, \phi)\, d\Omega + \int \tilde{S}_{vv}(\theta, \phi) \cdot f_{tvh}(\theta, \phi) f_{rvv}(\theta, \phi)\, d\Omega \right|^2 \right\rangle, \quad (9)$$

where Ω is the solid angle and $d\Omega = \sin\theta d\theta d\phi$. Using (9) we estimated the polarization isolation for DARR; it was found to be about 27 dB. This value of the polarization isolation is in good agreement with the atmospheric measurements.

d. Effect of the antenna patterns on the copolar and cross-polar correlation

The measurements of any element of the scattering matrix are influenced by the co- and cross-polar antenna patterns (Fig. 1). These antenna patterns determine the spatial structure of the copolar and cross-polar channel

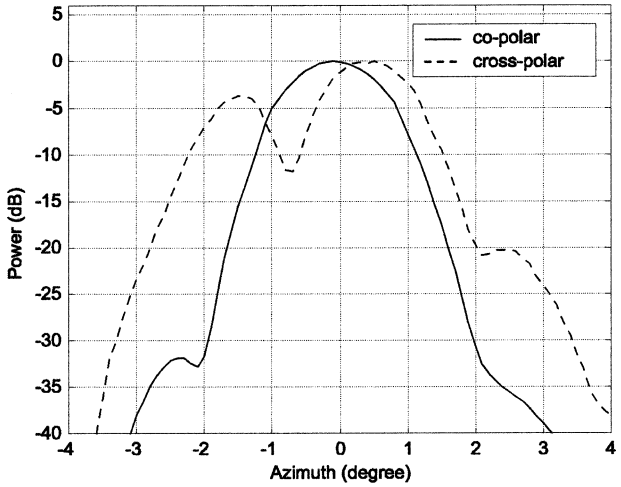

FIG. 2. Two-way antenna patterns (45° plane). The cross-polar pattern is normalized to have the same maximum value as the copolar pattern.

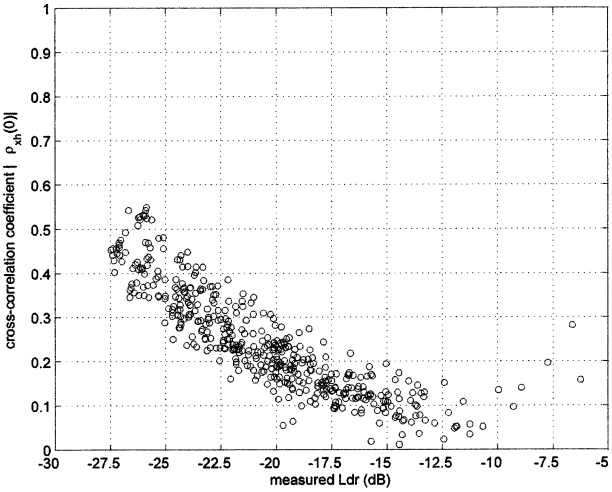

FIG. 3. Dependence of the cross-correlation coefficient $|\rho_{xh}(0)|$ on *Ldr* for precipitation measurements.

responses and are represented in the distortion matrices as f_{thh}, f_{tvv}, f_{rhh}, f_{rvv} for copolar patterns and f_{thv}, f_{tvh}, f_{rhv}, f_{rvh} for the cross-polar ones. In the cross-polar measurement of weakly depolarizing targets (most atmospheric objects), the influence of the cross-polar channel response is strong. Compensation for this influence is an important part of any calibration procedure. In a point target calibration procedure, the copolar and cross-polar channel responses are assumed to have no spatial dependences. However, in reality, this can be an erroneous assumption. From Fig. 1 and in more detail from Fig. 2 it can be seen that the co- and cross-polar antenna patterns have different shapes and as a result the observed volumes are also different.

The effect of the difference between these antenna patterns can clearly be seen in the observations of the magnitude of cross-correlation coefficient $|\rho_{xh}(0)| = |\langle M_{hh}M_{vh}^{*}\rangle/\sqrt{\langle|M_{hh}|^2\rangle\langle|M_{vh}|^2\rangle}|$ (or $|\rho_{xv}(0)|$) between copolar and cross-polar measurements of atmospheric objects. Figure 3 shows the dependence between the cross-correlation coefficient and the measured *Ldr* values. This figure presents data from six different measurements of light rain, in five cases with the radar pointed to the zenith and in one case at an 80° elevation angle. The figure shows measurement corresponding not only to the light rain but also to the melting layer and to the return from above the melting layer. In the light rain region, the measurements with $Ldr \approx -27$ dB had a signal-to-noise ratio for cross-polar measurements of about 15 dB. More details about the signal processing used to calculate the correlation coefficient can be found in section 4b.

It is commonly assumed that the correlation coefficient between pure copolar and cross-polar measurements of atmospheric objects is zero (Antar and Hendry 1985). Although recent studies by Ryzhkov (2001) have shown that in some cases the correlation coefficient can be nonzero, we do not expect that this effect will be significant for the zenith measurements of precipitation. So if this assumption is used, the further behavior of the scatterplot is clear and shows that with the increase of the *Ldr* values the correlation coefficient should decrease. However, the value of the cross-correlation coefficient for *Ldr* values close to -27 dB requires more explanation, as follows.

While the copolar measurements are mainly determined by the copolar response of the target, the cross-polar measurements are strongly affected by coupling between the polarization channels. Thus, if the measurements of the target are performed with $Ldr = -\infty$ dB, the expected value of $|\rho_{xh}(0)|$ from the point of view of point target calibration will be 1, since it does not have any spatial dependence and the measured cross-polar values are determined purely by the coupling from the copolar channel. But if the complete antenna patterns are taken into account, this value will be defined by the mismatch between the co- and cross-polar antenna patterns. In this case the co- and cross-polar measurements correspond to different radar volumes, and this results in the decorrelation between these two measurements.

To check whether this effect is strong enough to explain the observed values of the cross-correlation coefficient, we used the measured antenna patterns to calculate the measured $|\rho_{xh}(0)|$ for the case in which the copolar and cross-polar returns are completely correlated. To do this, we again used the 45° plane measurements and the assumption of rotational symmetry, as in section 3b. While this assumption is not generally valid for the cross-polar antenna patterns, it can be used for the purpose of this article, as shown below.

The two-dimensional distribution of the gain function of the cross-polar response of the antenna has four clear maxima: two in the 45° plane (see Fig. 2) and two in the 135° plane; for the other angles the cross-polar gain becomes smaller, reaching its minimum in the main

planes. As a result, if we used rotationally symmetric patterns obtained from the 45° plane antenna pattern, the intersection between the radar volumes for the copolar and cross-polar measurements is larger than in reality; hence we overestimate the correlation between the copolar and the cross-polar reflections. If the estimated magnitude of the correlation coefficient is significantly smaller than unity it will prove our hypothesis.

Let us calculate the correlation coefficient between cross-polar and copolar signals. By using (7), the received average power of copolar reflections can be written as

$$\langle M_{hh}M_{hh}^{*}\rangle = \iint \langle \tilde{S}_{hh}(\theta,\phi)\tilde{S}_{hh}^{*}(\theta',\phi')\rangle \times f_{thh}(\theta,\phi)f_{rhh}(\theta,\phi) \times f_{thh}(\theta',\phi')f_{rhh}(\theta',\phi')\,d\Omega\,d\Omega'. \quad (10)$$

We should note that due to the fact that reflections from different volumes are uncorrelated, we have that $\langle \tilde{S}_{hh}(\theta,\phi)\tilde{S}_{hh}^{*}(\theta',\phi')\rangle = 2\sigma_{\Omega}^{2}\cdot\delta(\theta-\theta',\phi-\phi')$, where $2\sigma_{\Omega}^{2}$ is the power per unit solid angle. Then, assuming uniform beam filling, (10) can be rewritten as

$$\langle |M_{hh}|^{2}\rangle = 2\sigma_{\Omega}^{2}\int f_{thh}^{2}(\theta,\phi)f_{rhh}^{2}(\theta,\phi)\,d\Omega. \quad (11)$$

For the cross-polar averaged power we have

$$\langle |M_{vh}|^{2}\rangle = 2\sigma_{\Omega}^{2}\int f_{thh}^{2}(\theta,\phi)f_{rvh}^{2}(\theta,\phi)\,d\Omega + 4\sigma_{\Omega}^{2}\int f_{thh}(\theta,\phi)f_{rvh}(\theta,\phi) \times f_{tvh}(\theta,\phi)f_{rvv}(\theta,\phi)\,d\Omega + 2\sigma_{\Omega}^{2}\int f_{tvh}^{2}(\theta,\phi)f_{rvv}^{2}(\theta,\phi)\,d\Omega. \quad (12)$$

To obtain (12) we have assumed that $\langle |S_{hh}|^{2}\rangle = \langle |S_{vv}|^{2}\rangle$ and $(\langle S_{hh}S_{vv}^{*}\rangle)/(\sqrt{\langle |S_{hh}|^{2}\rangle\langle |S_{vv}|^{2}\rangle}) = 1$. Finally the covariance is

$$\langle M_{hh}M_{vh}^{*}\rangle = 2\sigma_{\Omega}^{2}\int |f_{thh}(\theta,\phi)|^{2}f_{rhh}(\theta,\phi) \times f_{rvh}^{*}(\theta,\phi)\,d\Omega + 2\sigma_{\Omega}^{2}\int f_{thh}(\theta,\phi)f_{rhh}(\theta,\phi) \times f_{tvh}^{*}(\theta,\phi)f_{rvv}^{*}(\theta,\phi)\,d\Omega. \quad (13)$$

Using (11), (12), and (13) we calculated the cross-correlation coefficient and found it to be equal to 0.74. As expected, this value is larger than the measured value of 0.5 (see Fig. 3), but it proves that mismatching of the antenna patterns can have a significant influence on $|\rho_{xh}(0)|$.

Based on the above-presented studies we can conclude that

- for the *Zdr* measurements, a common point target calibration can be used,
- polarization isolation and thus the coupling terms (δ_1 and δ_2) are strongly dependent on the complete antenna pattern.

4. Improvement of the polarimetric radar calibration procedure

a. Use of light-rain zenith measurements for improvement of the calibration

The results presented above show that the polarimetric radar calibration procedure based on point target measurements does not give an adequate description of the influence of the radar antennas on cross-polar properties of atmospheric echoes. It also indicates that if a point target calibration procedure is combined with the measurements of a known distributed target a much better description of the effect of the radar system on polarimetric measurements can be achieved. However, the main problem of this approach is the availability of a distributed target with known polarimetric characteristics.

The most obvious candidate for the role of a known distributed target is light rain measured with the radar pointing to the zenith. Generally we would expect that for this type of measurement the light rain will behave as a polarimetrically isotropic nondepolarizing target, meaning that the actual *Ldr* of light rain is much smaller than the antenna limit. However, this assumption can be violated in some special cases. It was shown by Ryzhkov et al. (1999) that hydrometeors can have a nonzero mean canting angle, which will result in nonzero *Ldr* values even for a vertically pointing radar. This is usually caused by wind shear or updraft effects. Another effect (Jameson and Durden 1996) that can contribute to the failure of our assumption is that large raindrops can oscillate (change their shape). The oscillation will result in an increase of the *Ldr* values. These two effects can restrict the use of light rain for calibration. A reduction of these effects is feasible, however.

The oscillation of raindrops as well as a nonzero canting angle mainly contribute to the changes of polarimetric properties of large raindrops. This can be efficiently reduced by applying Doppler processing. Furthermore, these effects were mainly seen for strong rain intensities (reflectivity above 30 dB*Z*), while we use only light-rain data with values of reflectivities not larger than 20 dB*Z* (Fig. 4).

b. Signal processing used for the estimation of the polarimetric properties of rain

Several signal processing algorithms were applied to reduce the influence of the following four effects:

- ground clutter,

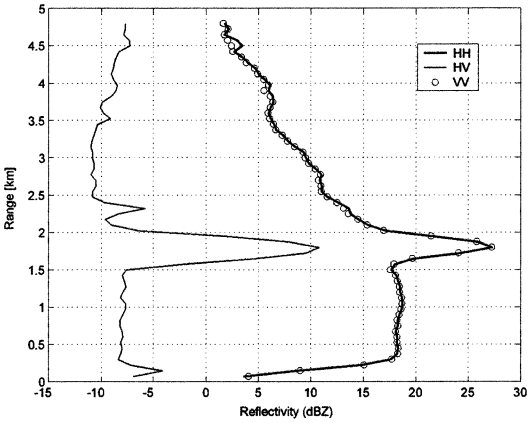

FIG. 4. A typical vertical profile of rain. Only the absolute calibration is applied.

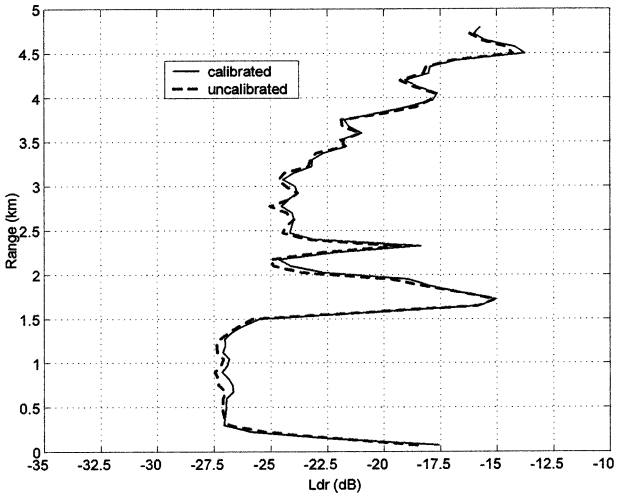

FIG. 5. *Ldr* profile of precipitation. The dashed line represents the uncalibrated *Ldr* and the solid line shows the calibrated *Ldr*. The point target calibration technique was used. Steady increase of *Ldr* values in the cloud region is caused by a decrease in SNR ratio.

- noise,
- change of the polarimetric properties of large raindrops, and
- staggered polarimetric measurements.

Since very accurate measurements of the small cross-polar signal are paramount for the calibration procedure the appropriate clutter suppression should be applied even to 90° elevation measurements of rain. The clutter suppression technique employed here is based on the use of the copolar correlation coefficient (Ryzhkov and Zrnić 1998; Moisseev et al. 2000) calculated for every Doppler resolution cell. For ground clutter these values are generally smaller than 0.7 and for atmospheric objects they are higher than 0.8. Thus, the Doppler cells that are contaminated by ground clutter can be successfully identified and suppressed. We should note that this processing also rejected cells with a poor signal to noise ratio (SNR). For further reduction of the noise, the averaged noise power was subtracted from all power measurements. Moreover, for all measurements presented in this paper averaging over 40 s was used.

In Fig. 4 the averaged vertical profiles of precipitation are given. It should be noted that in the cloud above the melting layer the signal-to-noise ratio decreases; as a result the SNR is almost unity for cross-polar measurements at the height of 4.5 km. This effect also causes a steady increase of *Ldr* values above the melting layer in Fig. 5. Therefore, for our analysis only data in the rain and melting layer were used, where SNR is better than 15 dB for the cross-polar measurements.

The possibility of large distorted drops affecting the processing was reduced by examining the behavior of *Zdr* and *Ldr* as functions of Doppler velocity (Unal et al. 2001). As a result, Doppler spectra, where changes in these parameters for different Doppler resolution cells are observed, were discarded.

Since DARR has only one receiver channel all covariances in the measured covariance matrix, $\mathbf{C}_m$, are obtained at nonzero time lag. Thus, it is necessary to estimate the values of this covariances at zero time lag. It can be shown that the difference between the cross-correlation calculated at zero time lag and at the time lag τ is an extra phase component $\omega\tau$ in the cross spectrum (Unal and Moisseev 2002). Thus, by compensating this phase difference on a calculated cross spectrum and performing inverse FFT we can obtain a very accurate estimate of the covariance at zero time lag [for more information see Unal and Moisseev (2002)]. Applying this step to all covariances in $\mathbf{C}_m$ we obtain a covariance matrix of precipitation as if all elements of the scattering matrix were measured simultaneously.

c. Improved calibration procedure and calibration results

From the above we can conclude that the point target calibration assumes that the antenna polarization states are completely polarized and thus they can be fully characterized by two 2×2 matrices, **T** and **R**. In particular, it has been shown that in the case of distributed target measurements the correlation coefficient between direct and coupling terms of antenna polarization states is not equal to unity, and thus the assumption that antenna polarization states are completely polarized is not valid. Thus, in order to describe such partially polarized states the combined second-order distortion matrix **D** should be used. Moreover, it should be noted that this distortion matrix cannot be determined from **T** and **R** alone, but needs to be corrected based on actual measurements of an extended target to take into account the full antenna pattern. In this section the procedure to improve calibration results for atmospheric studies based on measurements of light rain added to the results of the point target calibration is discussed.

As is shown above, the channel imbalance obtained

from the point target calibration is precise enough to retrieve the *Zdr* values. On the other hand, the cross-polar measurements are very sensitive to the calibration procedure and thus the polarimetric calibration should be modified in order to improve the accuracy of these measurements. Based on this, we can postulate that the channel imbalance f can be retrieved from the point target calibration while the light-rain measurements can be used to improve the cross-polar measurements.

To understand how to correct for the cross-polar errors, one needs to examine how M_{yx} and M_{xx} are affected by antenna pattern terms. For a target having $Ldr = -\infty$ dB, the measured voltage will be given as

$$M_{yx}(\theta, \phi) = f_{tyx}(\theta, \phi) f_{ryy}(\theta, \phi) S_{yy}(\theta, \phi) + f_{txx}(\theta, \phi) f_{rxy}(\theta, \phi) S_{xx}(\theta, \phi), \quad (14)$$

where $x, y = h, v$ (see Fig. 6 for an example of M_{vh} measurement). The copolar measurements, M_{xx}, of such a target will be defined as

$$M_{xx}(\theta, \phi) = f_{tyx}(\theta, \phi) f_{ryx}(\theta, \phi) S_{yy}(\theta, \phi) + f_{txx}(\theta, \phi) f_{rxx}(\theta, \phi) S_{xx}(\theta, \phi) \quad (15)$$

(see Fig. 6). Since for atmospheric echoes we do not expect *Zdr* to exceed 10 dB, meaning that $S_{hh} \sim S_{vv}$, and in the case of having a radar with a good polarization isolation (>20 dB) we can simplify the expression (15) by neglecting the term $f_{tyx} f_{ryx} S_{yy}$ and thus this expression can be rewritten as

$$M_{xx}(\theta, \phi) \simeq f_{txx}(\theta, \phi) f_{rxx}(\theta, \phi) S_{xx}(\theta, \phi).$$

If we now will consider the covariance $\langle M_{xx} M_{yx}^* \rangle$ we see that it is defined by the sum of the integrals with the elements under the integral sign that involve terms that are the first-order in $f_{xy}(\theta, \phi)$ [or $f_{xy}^*(\theta, \phi)$]. It should be noted that these elements are mainly responsible for the decorrelation between co- and cross-polar measurements. Of course there are other elements of the distortion matrix that include higher orders of the coupling terms and influence this covariance, but as we have shown above these elements can be neglected. In terms of the point target calibration the elements of the distortion matrix that are causing decorrelation are those that are first-order in δ_i (or δ_i^*), where $i = 1, 2$. Under the current assumption of reciprocity of the radar system, the co-cross-polar covariances should be equal for the measurements of light rain; this also is confirmed by our measurements. Therefore, the decorrelation between copolar and cross-polar measurements due to the antenna pattern is characterized by one correlation coefficient $|\rho_{xh}(0)|$. In order to take this decorrelation into account one should multiply the elements of the matrix $\mathbf{D}$ that are first-order in δ_i (or δ_i^*) by the cross-correlation coefficient $|\rho_{xh}(0)|$ obtained from the light-rain measurements. As a result we can obtain the modified distortion matrix, $\hat{\mathbf{D}}$, as

$$\hat{\mathbf{D}} = \begin{pmatrix} 1 & |\rho_{xh}(0)| & 1 & |\rho_{xh}(0)| & 1 & 1 & 1 & 1 & 1 \\ |\rho_{xh}(0)| & 1 & |\rho_{xh}(0)| & 1 & |\rho_{xh}(0)| & 1 & 1 & 1 & 1 \\ 1 & |\rho_{xh}(0)| & 1 & 1 & 1 & |\rho_{xh}(0)| & 1 & 1 & 1 \\ |\rho_{xh}(0)| & 1 & 1 & 1 & |\rho_{xh}(0)| & 1 & |\rho_{xh}(0)| & 1 & 1 \\ 1 & |\rho_{xh}(0)| & 1 & |\rho_{xh}(0)| & 1 & |\rho_{xh}(0)| & 1 & |\rho_{xh}(0)| & 1 \\ 1 & 1 & |\rho_{xh}(0)| & 1 & |\rho_{xh}(0)| & 1 & 1 & 1 & |\rho_{xh}(0)| \\ 1 & 1 & 1 & |\rho_{xh}(0)| & 1 & 1 & 1 & |\rho_{xh}(0)| & 1 \\ 1 & 1 & 1 & 1 & |\rho_{xh}(0)| & 1 & |\rho_{xh}(0)| & 1 & |\rho_{xh}(0)| \\ 1 & 1 & 1 & 1 & 1 & |\rho_{xh}(0)| & 1 & |\rho_{xh}(0)| & 1 \end{pmatrix} \cdot * \mathbf{D}, \quad (16)$$

where .* denotes the operator of element by element matrix multiplication.

A second step needed to improve the polarimetric calibration is to compensate for the difference between the polarization isolation estimations, (8) and (9). At first glance one can conclude that this can be done by solving (5) for δ_1 and δ_2. However, this solution is sensitive to the accuracy of f and it depends on the decorrelation compensation. Although the estimation of f from the point target calibration is accurate enough for the *Zdr* measurements, the order of magnitude of its error is comparable to the magnitudes of coupling terms δ_1 and δ_2. This means that the accurate solution of (5) for δ_1 and δ_2 is impossible. However, the polarization isolation estimates can be corrected simply by multiplying δ_1 and δ_2 by $\sqrt{\tilde{\rho}_a/\rho_a}$, where $\tilde{\rho}_a$ is the complete antenna polarization isolation and is equal to $1/Ldr$ from the light-rain measurements, and ρ_a is the point target isolation from (8). By doing so we keep the phases of δ_1 and δ_2 and the ratio δ_1/δ_2 as determined from point target calibration measurements and we adjust the amplitudes of the coupling terms to include the complete antenna pattern gain distribution. It should be noted that this step of the correction applies to each factor of δ_1 and δ_2 in the distortion matrix, $\hat{\mathbf{D}}$, and not just to the terms that are the first-orders in δ_1 and δ_2. It is most

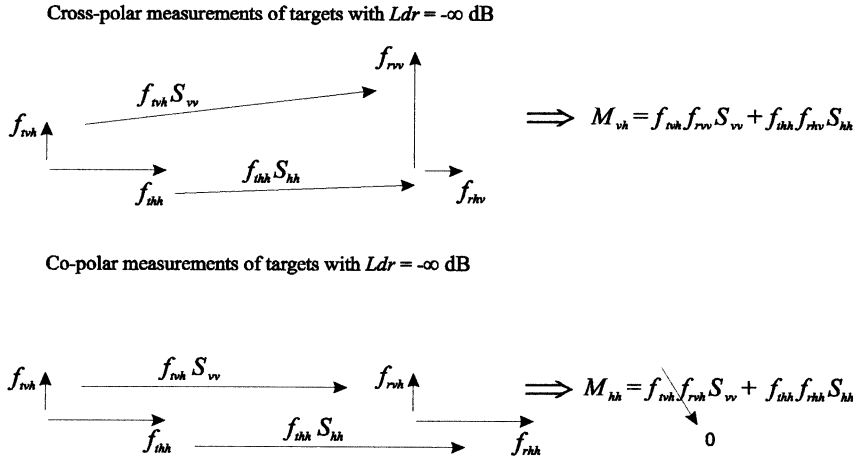

FIG. 6. A schematic graph showing the effect of the antennas on copolar (hh) and cross-polar (vh) measurements of a target with $Ldr = -\infty$ dB. It should be noted that under the normal circumstances of atmospheric measurements where $S_{hh} \sim S_{vv}$ the copolar measurements are mainly determined by the $f_{thh}f_{rhh}S_{hh}$ since $f_{tvh}f_{rvh}S_{vv}$ is at least two orders of magnitude smaller.

simply implemented by correcting the δ_i terms ($i = 1, 2$) in the transmission matrix $\mathbf{T}$ of Eq. (3), or in the 3×3 matrix of Eq. (4), from which $\mathbf{D}$ is determined.

These two simple procedures allow us to compensate for some discrepancy between the point target calibration and the measurements of extended targets. Of course, the assumptions underlying the current polarimetric calibration might not be valid for all cases; however, the use of these assumptions allows us to improve the polarimetric calibration method significantly. Moreover, these assumptions are less strong than the ones used when the point target calibration is applied, and thus it is implied that polarimetric characteristics of the antenna are solely defined by the polarimetric properties at the boresight direction.

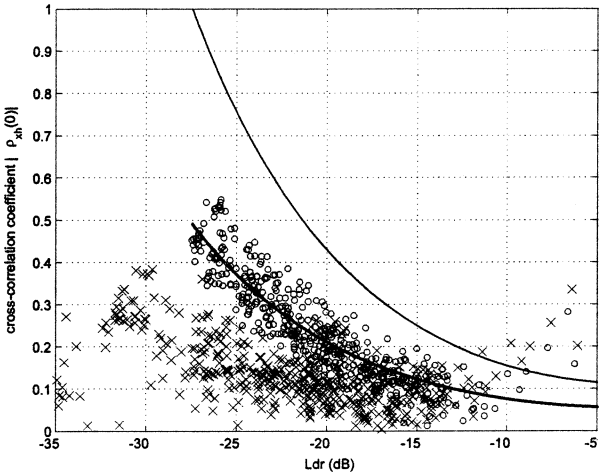

FIG. 7. The magnitude of cross-correlation coefficient between cross- and copolar measurements as a function of *Ldr*. The thin solid line shows prediction of this behavior if no decorrelation compensation is applied. The thick solid line represents prediction obtained from the final calibration model. The o-shaped markers show the behavior of the correlation coefficient before calibration (same as Fig. 3) and the x-shaped markers show the behavior of the correlation coefficient $|\rho_{xh}(0)|$ after the calibration.

In total six precipitation measurements were used to demonstrate the performance of the improved polarimetric calibration method. Two measurements were carried out on 27 November 1997 and the other four on 23 December 1997. Five of these measurements were obtained with the radar pointing to the zenith and one with a radar elevation angle of 80°.

In Fig. 5 one of the zenith measurements is used to show the result of the point target calibration procedure. It can be seen that the *Ldr* values have hardly changed after the calibration.

The scatterplot of the cross-correlation coefficient between cross- and copolar measurements as a function of the *Ldr* values obtained for all the measurements is shown in Fig. 7. Also two curves that represent the predicted behavior of the correlation coefficient are shown; the thin line shows the predicted behavior of $|\rho_{xh}(0)|$ if no decorrelation compensation is applied to the estimate of the combined distortion matrix and the thick line shows the prediction that is obtained when the decorrelation compensation (16) is applied. These two lines are obtained by applying the combined distortion matrices, $\mathbf{D}$ and $\hat{\mathbf{D}}$, with and without decorrelation compensation, to the modeled covariance matrix of precipitation, as

$$\mathbf{c}_m = \mathbf{D}\mathbf{c}_s \quad \text{or} \quad \mathbf{c}_m = \hat{\mathbf{D}}\mathbf{c}_s,$$

where the covariance matrix, $\mathbf{C}_s$, is given as follows:

$$\mathbf{C}_s = \begin{pmatrix} 1 & 0 & 1 \\ 0 & 10^{Ldr/10} & 0 \\ 1 & 0 & 1 \end{pmatrix}, \tag{17}$$

TABLE 1. Calibration parameters used to calculate the distortion matrices $\mathbf{D}$ and $\hat{\mathbf{D}}$.

	No decorrelation compensation ($\mathbf{D}$)	With decorrelation compentation ($\hat{\mathbf{D}}$)
f	$0.99 \cdot \exp(-i \cdot (87.5/180)\pi)$	$0.99 \cdot \exp(-i \cdot (87.5/180)\pi)$
δ_1	$0.0422 \cdot \exp(i \cdot (9/180)\pi)$	$0.0422 \cdot \exp(i \cdot (9/180)\pi)$
δ_2	$0.0450 \cdot \exp(i \cdot (162/180)\pi)$	$0.0450 \cdot \exp(i \cdot (162/180)\pi)$
$\lvert\rho_{xh}(0)\rvert$	1	0.49

and the *Ldr* values vary from −60 to −5 dB. The calibration parameters that were used to calculate $\mathbf{D}$ and $\hat{\mathbf{D}}$ are given in Table 1, it should be noted that in both cases the second step of the calibration correction is applied, namely the δ_i terms ($i = 1, 2$) are multiplied by $\sqrt{\tilde{\rho}_a/\rho_a}$. As we have discussed earlier the expected value of the co-cross-polar correlation coefficient for atmospheric echoes is zero; this is also is assumed in (17). Moreover, we also have shown that the bias of the measured correlation coefficient is caused by the imperfections of the radar. Naturally any calibration procedure should predict the behavior of the measurands. It can be seen, however, that if no decorrelation compensation is used, the prediction, calculated from $\mathbf{c}_m = \mathbf{D}\mathbf{c}_s$ and (17), gives wrong estimates of the measured correlation coefficient. On the other hand, the modified distortion matrix $\hat{\mathbf{D}}$ gives the right estimate of the uncalibrated correlation coefficient behavior and follows the scatterplot of the measured uncalibrated $|\rho_{xh}(0)|$, which is depicted by o-shaped markers, as shown in Fig. 7. Moreover, if we estimate the co-cross-polar correlation coefficient from our measurements by applying the new calibration procedure,[1] by computing $\mathbf{c}_s = \hat{\mathbf{D}}^{-1}\mathbf{c}_m$, we obtain a less biased estimate of the correlation coefficient, as shown by x-shaped markers. The other important conclusion that we can draw from this figure is that if the co-cross-polar correlation coefficient is used for the description of the media, extreme care should be taken. As we can see, even for *Ldr* values as high as −15 dB (Fig. 7) the correlation coefficient $|\rho_{xh}(0)|$ has a nonnegligible bias.

In Fig. 8 the scatterplot of the resulting *Ldr* values for all six precipitation measurements is shown. This figure shows that the proposed calibration procedure gives an improvement of about 7 dB in antenna isolation. It also shows that uncalibrated *Ldr* values have a bias of more than 1 dB for all measurements of the targets with the actual *Ldr* values of less than −20 dB. The result of the new polarimetric calibration is also demonstrated on the single precipitation profile, measured with the radar pointing to the zenith, as shown in Fig. 9. We can see that the calibration has a nonnegligible effect on rain measurements. Moreover, we also can observe that the measurements of the melting layer are hardly influenced by the procedure. That is expected since the melting layer is a depolarizing target with *Ldr* values of about −15 dB and as is shown in Fig. 8 the effect of the calibration on *Ldr* estimations of such targets is small.

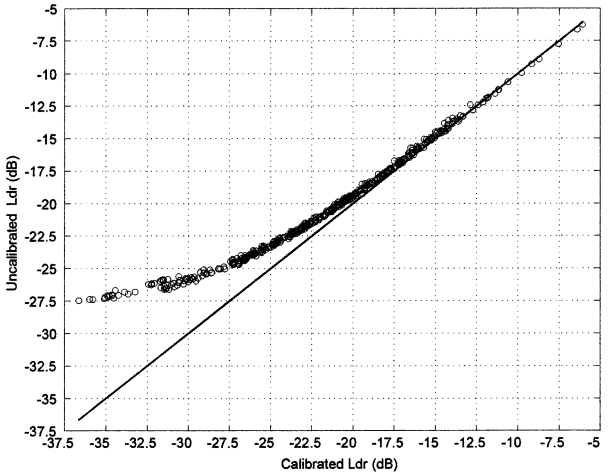

FIG. 8. Uncalibrated *Ldr* values of different precipitation measurements as a function of the calibrated *Ldr*. The solid line is given to facilitate the interpretation of the graph and shows a one-to-one relation between the calibrated and uncalibrated *Ldr* values.

5. Summary and conclusions

In this article the effect of complete antenna patterns on the polarimetric measurements of atmospheric phe-

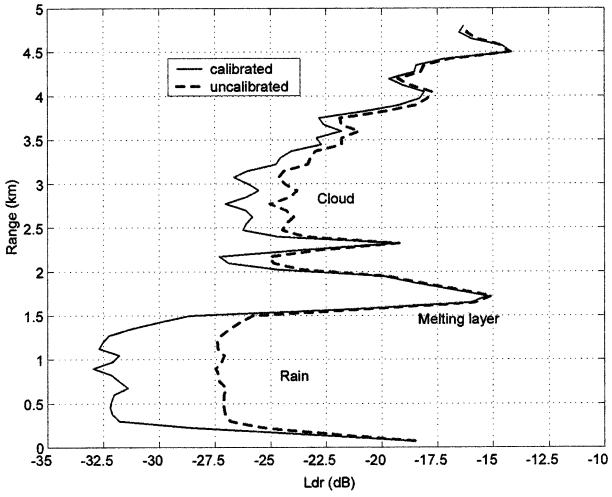

FIG. 9. Comparison between calibrated *Ldr* and uncalibrated *Ldr* values for a typical vertical precipitation profile. The improved polarimetric calibration procedure is used.

[1] Although one does not always need to compute all the elements of $\mathbf{c}_s$, in principle all the elements of the measured covariance vector $\mathbf{c}_m$ should be used for computing any element of $\mathbf{c}_s$. However, in some cases the calibration procedure can be significantly simplified. For copolar measurements a sufficiently accurate estimate of any copolar-related element of $\mathbf{c}_s$ can be estimated only by using measured copolar covariances and average copolar powers in $\mathbf{c}_m$. An accurate estimate of any cross-polar-like element of $\mathbf{c}_s$, on the other hand, will require measurements of all nine elements of $\mathbf{c}_m$. For more detailed analysis of errors that one would introduce by using only a few elements of $\mathbf{c}_m$, consult the magnitudes of the elements of the matrix $\hat{\mathbf{D}}^{-1}$.

nomena was analyzed. This study is based on the use of the measured antenna patterns as well as on the analysis of the precipitation measurements with DARR. The goal of this paper was to investigate the sensitivity of the polarimetric calibration to complete antenna patterns for atmospheric radars. It was shown that the common polarimetric calibration techniques, which imply that the polarimetric imperfection of a radar can be described from the measurements of known targets located at the boresight direction of the antenna, are not valid for the polarimetric measurements of atmospheric objects. The limitation of this assumption can clearly be seen in cross-polar measurements. It was also demonstrated that due to the antenna effects, both the *Ldr* values and the co-cross-polar correlation coefficient $|\rho_{xh}(0)|$ values are biased. This means that due to imperfection of the polarization channels, below about -20 dB the *Ldr* measurements have a nonnegligible bias for DARR. The co-cross-polar correlation coefficient has a bias of more than 0.1 even for the melting-layer measurements with *Ldr* values of -15 dB.

Based on this study a new polarimetric radar calibration procedure is proposed. This new calibration method uses light-rain measurements in order to take into account the extended nature of weather echoes. This combination of a point target calibration method and light-rain measurements has led to a substantial improvement in the cross-polar measurements of atmospheric objects. This improvement mainly manifests itself in an increase of sensitivity of the cross-polar measurements by more than 7 dB and in a reduction of the effects of the antenna on the co-cross-polar correlation coefficient $|\rho_{xh}(0)|$ measurements.

It should be noted, however, that the obtained data should carefully be analyzed; this is needed because polarimetric measurements are affected not only by an imperfection of the polarization channels, but also by noise, variance of the estimates of a covariance matrix elements, time changes of radar system characteristics, etc. All these effects can influence the performance of the polarimetric calibration and should be the topic of a future research. Therefore in our opinion the proposed calibration procedure should mainly be used to evaluate errors that are introduced by a system to polarimetric measurements and not to make attempts to measure *Ldr* below the antenna limit. Another use of this calibration procedure is to decrease the bias in the *Ldr* and $|\rho_{xh}(0)|$ estimates, which, as have been shown, is rather large even for the polarimetric measurements above the system limit.

Acknowledgments. The authors wish to thank the anonymous reviewers for their valuable comments. Especially the authors would like to acknowledge the contribution of one of the reviewers whose comments have greatly helped to clarify the manuscript.

REFERENCES

Antar, Y. M. M., and A. Hendry, 1985: Correlation measurements in precipitation at linear polarization using dual-channel radar. *Electron. Lett.,* **21,** 1052–1054.

Aubry, P., and J. H. Zijderveld, 1999: TARA reflector radiation pattern measurements. Tech. Rep. S010-99, IRCTR, Delft University of Technology, 33 pp.

Blanchard, A. J., and B. R. Jean, 1983: Antenna effects in depolarization measurements. *IEEE Trans. Geosci. Remote Sens.,* **21,** 113–117.

Doviak, R. J., and D. S. Zrnić, 1993: *Doppler Radar and Weather Observations.* Academic Press, 562 pp.

Hubbert, J. C., and V. N. Bringi, 2001: Estimation of polarization errors from covariance matrices of CSU-CHILL radar data. *Proc. 30th Conf. on Radar Meteorology,* Munich, Germany, Amer. Meteor. Soc., 44–46.

Jameson, A. R., and S. L. Durden, 1996: A possible origin of linear depolarization observed at vertical incidence in rain. *J. Appl. Meteor.,* **35,** 271–277.

Ligthart, L. P., and L. R. Nieuwkerk, 1980: FM-CW Delft atmospheric research radar. *IEE Proc. F. Commun. Radar Signal Process.,* **127,** 421–426.

McCormick, G. C., 1981: Polarization errors in a two-channel system. *Radio Sci.,* **16,** 67–75.

Moisseev, D., C. Unal, H. Russchenberg, and L. Ligthart, 2000: Doppler polarimetric ground clutter identification and suppression for atmospheric radars based on co-polar correlation. *Proc. 13th Int. Conf. on Microwaves, Radars, and Wireless Communications,* Wroclaw, Poland, Telecommunications Research Institute (PIT), 94–97.

Ryzhkov, A. V., 2001: Interpretation of polarimetric radar covariance matrix for meteorological scatterers: Theoretical analysis. *J. Atmos. Oceanic Technol.,* **18,** 315–328.

——, and D. S. Zrnić, 1998: Polarimetric rainfall estimation in the presence of anomalous propagation. *J. Atmos. Oceanic Technol.,* **15,** 1320–1330.

——, ——, E. Brandes, J. Vivekanandan, V. Bringi, and G. Huang, 1999: Characteristics of hydrometeor orientation obtained from radar polarimetric measurements in a linear polarization basis. *Proc. IGARSS'99,* Hamburg, Germany, IEEE Geoscience and Remote Sensing Society and Cosponsors, 702–704.

Santalla, V., Y. M. M. Antar, and A. G. Pino, 1999: Polarimetric radar covariance matrix algorithms and applications to meteorological radar data. *IEEE Trans. Geosci. Remote Sens.,* **37,** 1128–1137.

Sarabandi, K., and F. T. Ulaby, 1990: A convenient technique for polarimetric calibration of single-antenna radar systems. *IEEE Trans. Geosci. Remote Sens.,* **28,** 1022–1033.

——, ——, and M. A. Tassoudji, 1990: Calibration of polarimetric radar system with good polarization isolation. *IEEE Trans. Geosci. Remote Sens.,* **28,** 70–75.

Unal, C. M. H., and D. N. Moisseev, 2002: Improved Doppler processing for polarimetric radars: Application to precipitation measurements. *Proc. URSI-F Open Symp. on Propagation and Remote Sensing,* Garmisch-Partenkirchen, Germany, URSI and DLR, CD-ROM.

——, R. J. Niemeijer, J. S. V. Sinttruyen, and L. P. Ligthart, 1994: Calibration of a polarimetric radar using a rotatable dihedral corner reflector. *IEEE Trans. Geosci. Remote Sens.,* **32,** 837–845.

——, D. N. Moisseev, F. J. Yanovsky, and H. W. J. Russchenberg, 2001: Radar Doppler polarimetry applied to precipitation measurements: Introduction of the spectral differential reflectivity. *Proc. 30th Conf. on Radar Meteorology,* Munich, Germany, Amer. Meteor. Soc., 316–318.

Zrnić, D. S., and A. V. Ryzhkov, 1999: Polarimetry for weather surveillance radars. *Bull. Amer. Meteor. Soc.,* **80,** 389–406.